

The work described was performed by Transportation Technology Center, Inc., a wholly owned subsidiary of the Association of American Railroads.

## Dynamic Analysis of Rail Grinding Templates

Scott Cummings and Stan Gurulé

[Transportation Technology Center, Inc. \(TTCI\)](#) analyzed the grinding templates for curved track currently in use by Class 1 railroads in North America. Particular emphasis was placed on the low rail templates because they tend to require the heaviest grinding effort, and a comparison of the templates used on low rails showed much variation. This *Technology Digest* (TD) describes the dynamic portion of the analysis while a companion TD covers the static portion of the analysis.<sup>1</sup>

### BACKGROUND

One of the primary drivers for rail grinding is the restoration of a desired cross-sectional rail profile shape. On the low rail in curved track, the railhead tends to wear into a flat shape which can allow the false flange of hollow worn wheels to contact the field side of the rail. This inhibits the desired steering effect produced by having a smaller rolling radius on the low rail wheel compared to the rolling radius of the high rail wheel. It also reduces the rail's geometric resistance to rolling over to the field side of the track.

Wheel/rail contact and steering mechanics result in lateral forces that tend to spread gage and roll the rail outward. Several factors act to resist rail roll: vertical wheel/rail forces produce a moment in the opposite direction, fasteners restrict rail base motions, and the torsional strength of the rail resists roll at any one particular location. If the wheel/rail lateral-to-vertical (L/V) force ratio exceeds the rail base-to-height (B/H) ratio, the roll resistance becomes completely reliant on fasteners and torsional strength. Thus, the greater the B/H ratio, the more stable the rail is against rollover. The traditional or Nominal B/H value, as reported by track measurement systems, is based only on the highest point of the rail profile. A Functional B/H value is determined by the center of contact between a wheel profile and a rail profile.<sup>1</sup> All references to B/H in this TD imply a Functional B/H except where noted. Both the L/V and the B/H value are largely dependent on the wheel/rail profiles and contact conditions.

### Key Findings:

- NUCARS® simulations showed that low rail grinding templates with a vertical field side relief of at least 0.070 inch produce profiles that generally performed well in the presence of hollow worn wheels with regard to the Functional base-to-height ratio (B/H), the B/H minus lateral-to-vertical force ratio (L/V), and contact stress.
- The simulations showed varied performance levels for grinding templates with vertical field side relief between 0.055 and 0.059 inch and poor performance for a grinding template with a vertical field side relief of 0.037 inch.
- A field side relief is more important than crown radius in grinding a low rail profile that tolerates hollow worn wheels.

NUCARS® is a registered trademark of Transportation Technology Center, Inc

## METHODOLOGY

Rail grinding templates for Class 1 railroads were obtained and overlaid on typically-worn low rail and high rail profiles. The alignment method used in this analysis has been described in detail in a previous TD (TD16-053) as "Method C (Range)."<sup>2</sup>

Eight low rail profiles were matched up with the corresponding high rail profile(s) and given an alphabetic designation corresponding with Nominal B/H values ranked in descending order (i.e., Profile A has the highest Nominal B/H value and so on). The appropriate high rail profile was matched with the corresponding low rail profile based on the track curvature.

## STATIC ANALYSIS SUMMARY

B/H values were calculated for each low rail profile matched up with a library of 604 wheelsets with hollow wear ranging from 1 to 4 mm. Figure 1 plots the vertical relief measured 0.25 inch from the field side of the rail as a function of crown radius and contains commentary from the static analysis regarding the relative effectiveness of the rail profiles in maintaining high B/H values in the presence of hollow worn wheels.

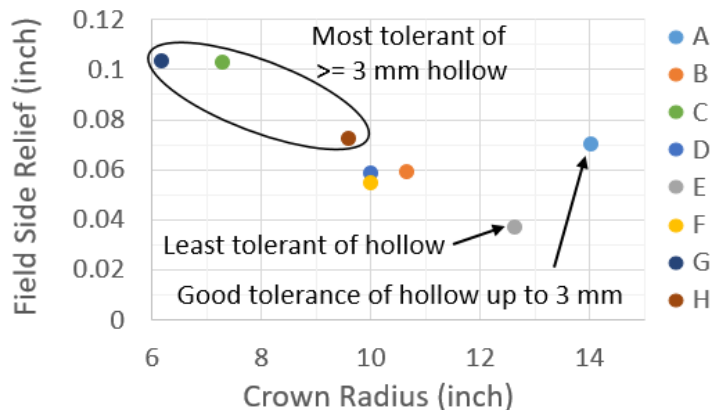


Figure 1. Low rail template crown radius and vertical field side relief

## DYNAMIC ANALYSIS

The following conditions were simulated using NUCARS<sup>®</sup> vehicle dynamics software:

8 rail pairs × 4 curves × 3 track gages × 3 wheel/rail friction conditions × 2 car weights × 5 wheelset profiles = 2,880 cases

Four curvatures were modeled: 1, 3, 6, and 10 degrees. Superelevations were set to provide a balanced condition near 25 mph, and all simulations were conducted at the balancing speed. Narrow, standard, and wide gage conditions were modeled at 56.25, 56.50, and 57.00 inches, respectively. Three wheel/rail friction conditions were modeled using the following coefficients of friction for the top of the rail and the gage face of the rail, respectively: dry (0.50, 0.50), flange lubrication (0.50, 0.20), and top-of-rail friction modifier plus flange lubrication (0.35, 0.20).

All simulations involved a grain hopper car with constant-contact side bearings and M-976 qualified trucks in new condition. The car was simulated fully loaded with a gross rail load of 286,000 pounds and empty with a tare weight of 63,000 pounds. Wheel profiles were selected to represent one wheelset each with 0-, 1-, 2-, 3-, and 4-mm hollow wear on the low rail wheel. The same high rail wheel profile with 0.75-mm hollow wear was used in every simulation. Each simulation used the same wheelset profiles at all four axle positions in the car. All reported results pertain to the low rail wheel of the lead axle. Though the dynamic analysis used significantly fewer wheelset profiles (five) than the static analysis (604), this analysis did include other interacting variables that influenced wheel/rail contact positions and forces (curvature, gage, friction, and car load status).

Figure 2 shows the B/H values for each rail pair on the 10-degree curve averaged over all other parameters simulated as a function of hollow wheel wear. The 10-degree curve was selected for this figure because flanging on the high rail is expected. Although these trends look similar to the B/H values generated in the static analysis, in the dynamic analysis there was reduced differentiation between rail profiles because the average B/H values did not drop below 0.25. The dynamic analysis B/H values corresponded to the wheelset position during steady-state curving, while the static analysis used the lateral wheelset position that produced the smallest B/H value. B/H values of less than 0.41 indicate the occurrence of wheel/rail contact on the field side of the rail centerline.

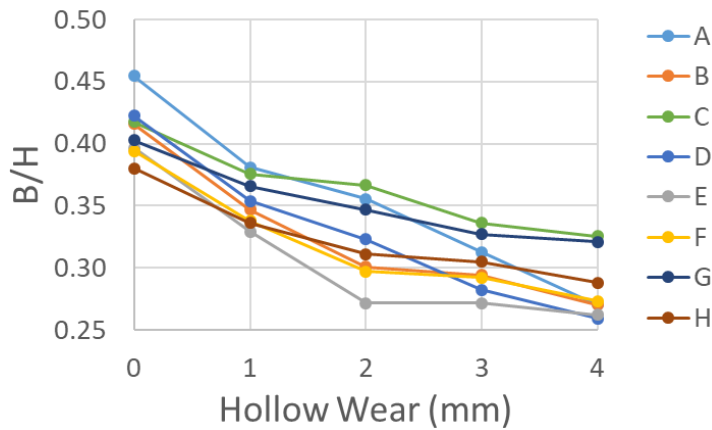


Figure 2. Low rail average B/H values for the 10-degree curve

Track gage has an influence on B/H values as hollow wear increases. Average B/H values for the 4 mm hollow wheel on the 10-degree curve for all rail profiles were 0.26, 0.27, and 0.32 for narrow, standard, and wide gage, respectively. This was because the false flange contacted the low rail nearer the center of the rail head when the high rail wheel was flanging on wide gage track. On narrow gage track, the low rail contact position was more dependent on the low rail profile. Profiles A, B, D, E, and F were more sensitive to narrow gage combined with heavy hollow wear in comparison to profiles C, G, and H. B/H values were fairly unaffected by wheel/rail friction conditions. Figure 3 shows the values of low rail B/H minus single wheel L/V averaged for all other parameters considered as a function of wheel hollow wear.

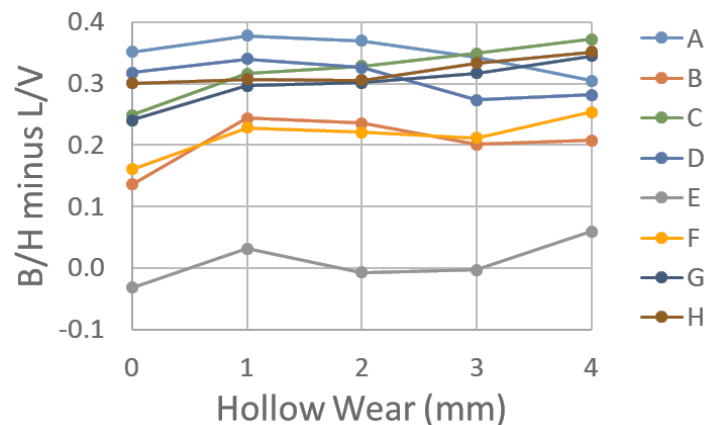


Figure 3. Low rail average B/H minus single wheel L/V values

Values less than 0.0 indicate that rail roll resistance is reliant on fasteners and rail torsional strength rather than the geometry of the rail. Profiles A, C, D, G, and H showed the best performance in this metric with no average values below 0.24. Profiles B and F performed similarly with average values between 0.14 and 0.25. Though not shown in Figure 3, Profiles B and F performed similarly to A, C, D, G, and H on the 1- and 3-degree curves but showed much lower values on the 6- and 10-degree curves. Profile E, with its relatively large crown radius and low field side relief, was the poorest performer with regard to the B/H minus L/V metric.

Figure 4 shows the contact stress due to the vertical, lateral, and longitudinal force components generated in the low rail contact patch and averaged for all other parameters as a function of wheel hollow wear. Contact stress can influence rail wear, rolling contact fatigue, and material flow. Many of the rail profiles performed similarly with some notable exceptions. Profile E generated high contact stress with wheels of at least 2 mm hollow due to contact between the false flange and the field corner of the low rail. The same was true of Profile D and the 4-mm hollow wheel. Profile G had a relatively sharp curvature transition between the top of the rail and the field side runoff slope that came into high stress contact with the 2- and 3-mm hollow wheels, but not the 4-mm hollow wheel due to its false flange being slightly further toward the front rim face.

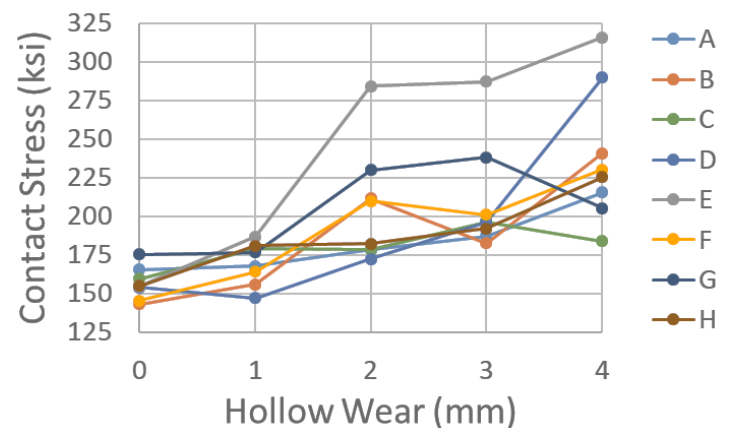
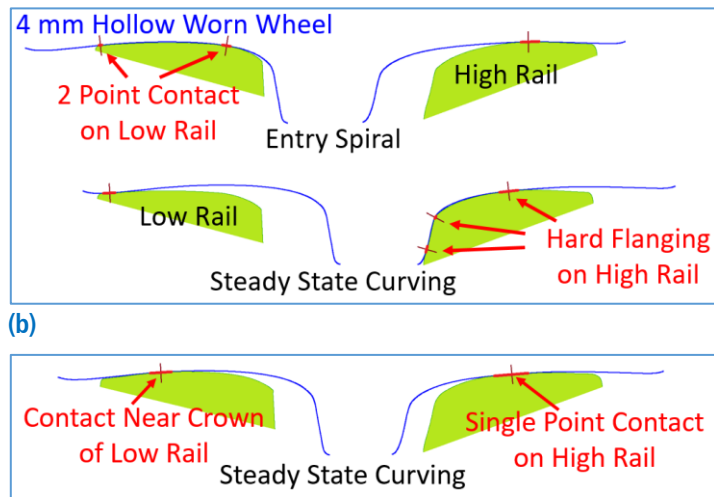


Figure 4. Low rail average contact stress values

## DISCUSSION

Profiles C and G may have been grinding more metal than necessary given that field side relief of over 0.1 inch does not significantly reduce contact stresses compared with Profiles A and H which had field side relief of approximately 0.070 inch.

An explanation of the causes for the performance of Profile E is warranted. The top portion of Figure 5 shows the contact conditions for Profile E at the high and low rails when matched with the 4-mm hollow worn wheelset in a 6-degree curve. In the curve entry spiral, the wheelset shifted laterally in an attempt to generate a sufficient rolling radius difference between the wheels. The low rail did not contact the most worn portion of the wheel tread with the smallest rolling radius. In the body of the curve, the wheelset shifted laterally into a hard flanging position, resulting in contact at the low rail field corner leading to a high L/V value and high contact stress on the low rail.



(b)  
 Figure 5. Wheel/rail contact for Rail Pair E (a) and Rail Pair C (b)

In contrast, the bottom portion of Figure 5 shows that the low rail profile of Rail Pair C allowed contact at any point on the railhead with the 4 mm hollow worn wheel. The wheelset was able to establish sufficient rolling radius difference between the wheels without flange contact on the high rail. This allowed a lower L/V value and a larger contact patch on the low rail giving lower contact stress.

## CONCLUSIONS

A dynamic analysis of the rail profiles produced by the grinding templates used by Class 1 railroads reinforced conclusions from the static analysis and added some additional insight. Profiles G and H had the lowest Nominal B/H values, yet were among the best performing profiles in the dynamic analysis showing that Nominal B/H is not necessarily a good metric for evaluating low rail tolerance of hollow worn wheels. Field side relief is more important than crown radius in grinding a low rail profile that tolerates hollow worn wheels. The four profiles with at least 0.070 inch of field side relief generally performed best in the dynamic analysis despite having a large range of crown radii (6.2 to 14.0 inches). Transitions between arcs should be as smooth as possible to avoid high contact stress such as observed with Profile G when matched with the 2- and 3-mm hollow wheels. Profile E did not perform as well as the others due to low rail field side relief less than 0.040 inch.

## References

1. Cummings, S., August 2020, "Static Analysis of Rail Grinding Templates," *Technology Digest* TD20-021, AAR/TTCI, Pueblo, CO.
2. Keylin, A. and S. Cummings. November 2016, "Comparison of Rail Grinding Template Alignment Methods." *Technology Digest* TD16-053, AAR/TTCI, Pueblo, CO.

For comments or questions about this publication, contact [Scott\\_Cummings@aar.com](mailto:Scott_Cummings@aar.com)

Disclaimer: Preliminary results in this document are disseminated by the AAR/TTCI for information purposes only and are given to, and are accepted by, the recipient at the recipient's sole risk. The AAR/TTCI makes no representations or warranties, either expressed or implied, with respect to this document or its contents. The AAR/TTCI assumes no liability to anyone for special, collateral, exemplary, indirect, incidental, consequential or any other kind of damage resulting from the use or application of this document or its content. Any attempt to apply the information contained in this document is done at the recipient's own risk. Unauthorized duplication or distribution is prohibited.